DOI: ADD DOINUMBER HERE

# Feature extraction from micro-tomography analysis of solid propellants

*Filippo Maggi* * *and Marco Bratti* †
*Politecnico di Milano*
*Dept. Aerospace Science and Technology, 34, Via La Masa, Milano, Italy*

## Abstract

The study of the microstructure in composite solid rocket propellants is mostly focused on the properties and placement of oxidizer and metal particles. Both combustion and mechanical properties are influenced by their size, shape, orientation, and surface-binder interaction. The investigation methods span from numerical simulation of casting, directional burning rate analysis, modeling of microstructure, and micro-tomography. This last investigation technique has always been considered an interesting non-destructive inspection method, though qualitative. High-quality imaging of solid propellant inner structure is not simple. Particles are close-packed each other, with small binder strips in between. Materials are characterized by different absorption capabilities, making artifacts and edge detection complex. In this respect, the paper presents some new developments at SPLab-POLIMI to inspect micro-tomography and extract information from a heterogeneous composite material. A discussion about image unsharpness will be reported with supporting data.

## 1. Introduction

Heterogeneity is a multi-scale problem, strongly influenced by the observation viewpoint. If we observe a wall of bricks from a large distance, the surface will appear uniform, the color homogeneous and we will not observe directional properties. When the observer gets closer to the wall, bricks will become evident. Whitish strips of cement will appear between the red color of the bricks, following preferential directions. The brick becomes the unit element of the wall, displaced in a precise geometrical order. The category of heterogeneous matter comprises a very wide number of common materials. Concrete, pressed powder pellets, asphalt, and solid propellants represent only few examples of intrinsically heterogeneous materials that manifest macroscopically homogeneous properties.

Composite solid propellant global characteristics are determined by their microstructure which, in turn, depends on the details of its composition. They are a mechanical mixture of solid ingredients in the shape of micrometric powders and an elastomeric matrix which gives mechanical consistency. The mixing action confers random-kind displacement of particles however a sort of order can be identified. Coarse oxidizer (in the range 200 μm to 400 μm) , fine oxidizer (about 10 μm to 20 μm), aluminum powder (typically, 15 μm to 30 μm), and a minor fraction of additives are arranged in pocket-kind structures where fuel-lean regions are surrounded by coarse oxidizer. The reader can find in the literature the classical Cohen's geometric vision and more recent pseudo-random approach by Maggi et al.[1,2]

A typical example of micro-scale influencing the macro-scale is represented by the overall packing factor of multimodal powders.[3] Even in presence of monomodal particles, variation of spatial organization causes a difference in volume of the global assembly and, thus, of the density. The same considerations can be done on propellants. The change in the oxidizer coarse-to-fine ration produces different global density. As an example these microstructure properties can alter the burning rate as an increment is observed for higher fraction of fine component. When we move from the scientific side to real implementation, the things become even more complex. The presence of voids, related to imperfection of the manufacture causes further decrease of the propellant density and the generation of a discontinuity in the medium, with consequent safety issues related to heat transfer and mechanical properties.

*filippo.maggi@polimi.it, Associate Professor, Space Propulsion Laboratory, corresponding author
†marco.bratti@mail.polimi.it, M.Sc. Student, Space Propulsion Laboratory

## 2. Microstructure in propellants and tomography

Even minimal details of the microstructure can cast their effect over the behavior of a propellant. For example, the production process of some types of BATES (ballistic test and evaluation system) motors have been found to influence the shape of the pressure trace. Numerical casting simulations demonstrated that the stress induced by the insertion of the mandrel for manufacturing the central perforation could be correlated to a local anomaly of the pressure trace.[5] Very likely, this localized stress has determined a minimal, though significant, alteration of the microstructure. The same problem was investigated experimentally confirming local burning rate variation across the web thickness.[6] Also shape and orientation of particles can be important. A numerical study by the CSAR group of the UIUC has shown that the orientation of non-spherical oxidizer may lead to change in burning rate.[7] In this paper, spherical particles have been virtually stretched to ellipses numerically obtaining different burning rates when the deformation was modified in combustion simulations.

X-ray computed tomography allows the inspection of material bulks. The technique is based on a set of X-ray back projections which reveal the radiographic absorption capability of a sample along a precise line of sight.[8] This technique can use five different geometric configurations. A common one is called "cone-beam" and is based on a point-wise X-ray source, a detector, and a sample placed in between. The source emits a conic beam and impinges upon the sensor after passing through the sample. There are two possible modes to operate this kind of instrument: in one case the sample is lodged on a rotating table while the instrumentation is fixed, in another case the sample is fixed while detector and source rotate accordingly. Finally, an algorithm merges the information of a complete 360 ∠ rotation and produces a three-dimensional absorption map.

The use of tomography in solid propellants was used to inspect qualitatively the propellant microstructure by Gallier[9] and by Collins and co-authors.[10] More recently, Maggi and Garg inspected also the degradation of single ingredients after thermal cycles (namely, cracks inside single particles of ammonium nitrate).[11] An example of two-dimensional cut of an AP-based propellant micro-tomography is reported in Figure 1. The image shows clearly the presence of different ingredients, given their contrasting X-ray absorption capability. Aluminum powders appear as bright spots, being a metal with relatively high density with respect to the other components. The oxidizer has an intermediate gray scale. The coarse particles are well defined in the reported image. The binder is the most difficult part to detect. It may contain a dispersion of fine oxidizer having size in the order of the scan resolution. Moreover, carbon-based plastics feature low absorption capability.

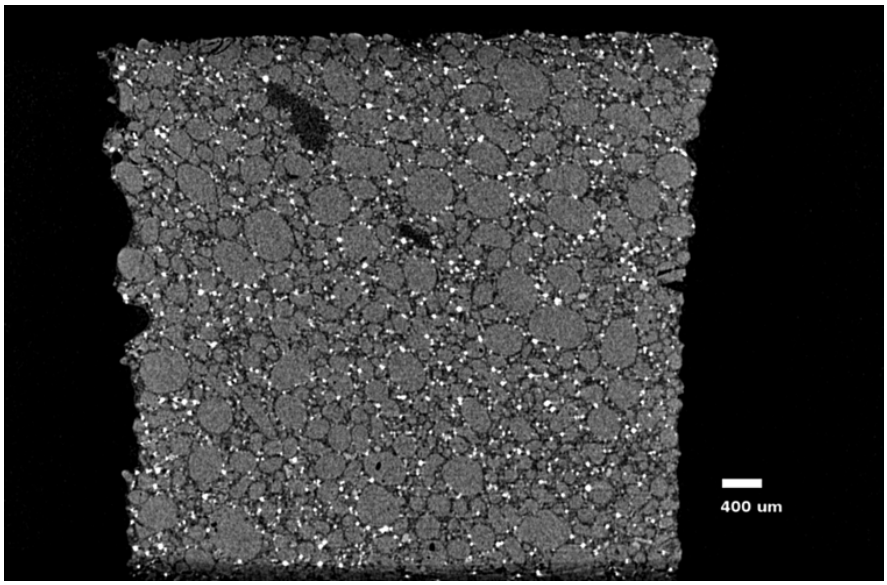


Figure 1: Micro-tomographic view of a metalized solid propellant

## 3. Considerations on image quality

Images obtained directly from the tomography are rarely a perfect representation of the object microstructure, since they are usually affected by various factors such as optical transfer function, scatter, noise, unsharpness, artifacts, ...[12] Image analysis and processing generally refers to a series of digital manipulations improving their quality and aiming

at extracting representative information (e.g. numerical data) from them. A good discussion on the topic was published by Schlüter et al.[13] CT image analysis and processing usually consists in the following steps, even though some of them may be skipped for some purposes:

- Correction of defects: filters for quality increment, algorithms acting on scattering, artifacts, and noise are used for the reduction and mitigation of the imperfections present in the tomographic images.[14,15]
- Enhancement of important details: emphasis of the main features of interest and removal or suppression of other information that do not represent the main interest of the analysis. Hence, what remains results to be more accessible for human interpretation and more isolated for eventual successive measurements. The application of filters for contrast enhancement and image sharpening are the basis of this step.[16]
- Binary representation: with thresholding and segmentation the gray-scale images are converted into binary ones (black/white representation) and are divided into multiple parts. These actions are performed in order to separate the aspects to be analyzed (usually composed by the white pixels) from the background (usually composed by the black pixels). A large number of techniques of image thresholding and segmentation are available in the literature.[17]
- Object recognition: process for identifying specific objects in digital images. It relies on matching, learning or pattern algorithms which use appearance-based or feature-based techniques.[18]
- Quantitative analyses: this step is strictly dependent on the final goal of the object tomographic inspection.

The use of quantitative tomographic characterization of a composite propellant microstructure is not straightforward as a standard qualitative view. If the intention resides in the characterization of particles we should remember that, according to Barrett, particles are characterized completely by size, shape, and surface finishing.[19] This is valid when uniform material is expected. A more detailed characterization should consider the internal composition (e.g. defects or multiple materials) and, when the particle is embedded in a heterogeneous material, also the orientation. Accuracy of size and shape is a matter of both software and hardware reasons and its quantification is addressed by the German directive VDI/VDE 2630.[20] Some of the hardware reasons can be found in detector, X-ray source, movement accuracy, sample stability, scanning conditions. Radiography correction, reconstruction algorithm, surface identification, thresholding are some of the software reasons. It should be underlined that said directive is pushing the machine to its best performance as it works with simplified geometries, ideal material compositions, as well as smooth and regular surfaces. Because of the high number of particles, varying size, type of materials, proximity, and random mixing, the real accuracy of the entire scanning process is the real bottleneck and can hardly reach the nominal features of the machine.

## 4. Reference tomography

In this paper a propellant tomography (internal identification no. SPL-CT-064) was considered for reference. The 3D reconstruction is reported in Fig. 2. The sample is a stack of two non-aluminized solid propellant charges loaded with ammonium nitrate oxidizer of 6 mm diameter and 8 mm height. The propellant was produced with non-optimal procedure. It was mixed by hand without vacuum cycle. The composition was made by HTPB binder, non-stabilized ammonium nitrate produced by Yara (volume mean diameter 386 μm), and phase-stabilized ammonium nitrate (volume mean particle size 204 μm) prilled with the addition of potassium nitrate (stabilizer) by ICT Fraunhofer Institute, Karlsruhe, Germany.

The tomography was performed using a X-25 X-ray micro-tomographic machine by NSI. The X-ray source was operated at 60 kV and 25 μA, granting a magnification factor of 6.22 and a voxel resolution of 11.0(96) μm. It should be considered that the apparatus is capable of a nominal certified resolution of 2 μm.[21] The reconstruction of the image was performed using a proprietary software supplied with the machine introducing fine-tuning corrections for rotational axis identification and beam hardening. A set of 8 bit gray-scale output images have been obtained from slicing the tomography along one of the machine axes.

## 5. Qualitative feature extraction

The access to the bulk microstructure with qualitative inspection supplies initial information about the sample. Figure 3 shows one slice of the reference tomography after reconstruction and extraction from the 3D data set. The resolution and the sensitivity of the analysis is enough to identify some important features for quality assessment and production process analysis. The slice is showing that all particles have rounded shapes. Fragmentation of crystals due to mixing

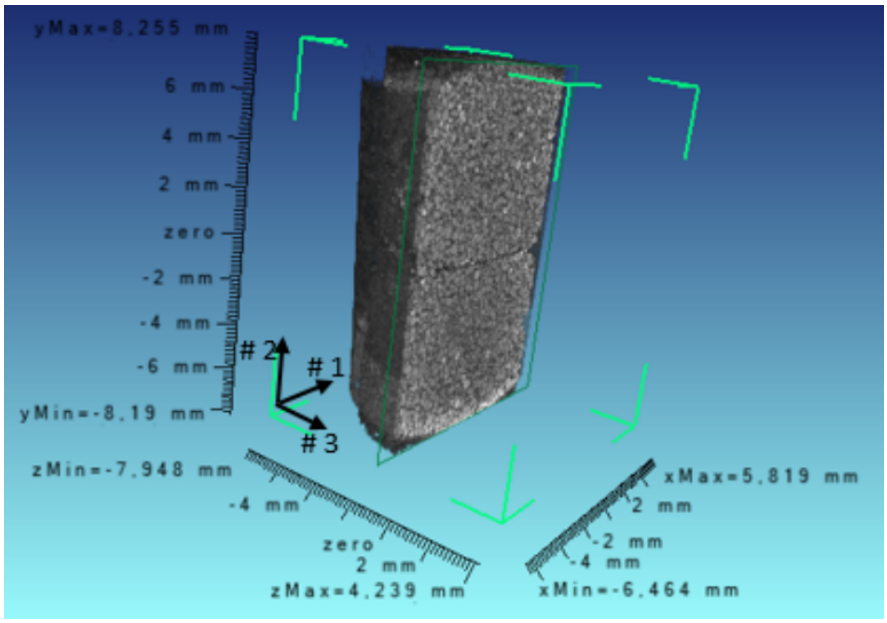


Figure 2: Three-dimensional representation of tomography SPL-CT-064.

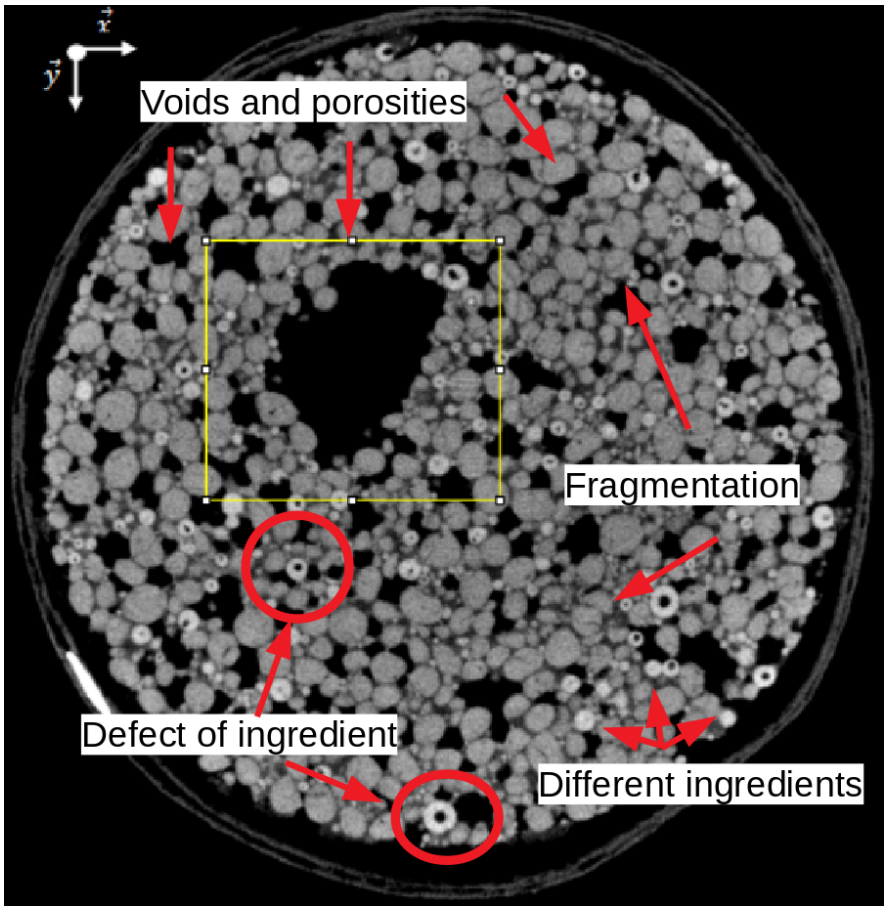


Figure 3: Qualitative observation of a tomographic 2D slice

is not evident. Apparently there are groups of particles with bean-kind smooth aspect and others with spherical shape. Since the production technique of the ingredients is known, it can be inferred that the first ones are mainly non-stabilized ammonium nitrate particles while the latter are the prilled ones.

In the image different levels of porosity are identified by the black color. A macroscopic void is visible in the center of the image, highlighted by a yellow square. All around a number of micro-pores are also visible, having typical size below the one of the oxidizer. Wetting issues as well as non-uniform mixing are clearly identified by this tomographic setup. Defects of the ingredients can be identified as well. In the red circle the reader can observe another void. In this case, the production of the propellant is not responsible for those. These defects seem to affect only rounded particles and may be generated by the presence of voids after prilling. The resolution of this scan enables also the identification of non-stabilized ammonium nitrate fragmentation. This is very likely caused by thermal cycle of the ingredient itself and by the accumulation of damage.[11] The fracture is only faintly visible under these scanning conditions. Finally, the scan shows the ammonium nitrate particles colored by two different gray scale levels. Most of the particles are depicted by darker gray with respect to lighter gray of the prilled ones. This fact allows the identification of the ingredient, crystal by crystal. Very likely, the prilling process and the addition of the stabilizing additive is modifying the X-ray absorption capacity of the ingredient.

## 6. Commencing quantitative feature extraction

### 6.1 Source of information

In a 3D problem, volume and surface area are the two major sources of information for particle characterization. Volume-based and surface-based factors can be used to report about size and shape. A combination of volume and surface area information can be used as well. Surface-based factors are generally sensitive to small changes of the shape, being capable of capturing small changes. They can be affected by the presence of noise or other inaccuracies, though. Volume-based factors are less sensitive to small changes. They represent a more robust characterization method in presence of noise, though less effective for detection of small details.[22]

The correct representation of particles properties requires the proper identification of the edge between contacting particles or between particle and surrounding medium. Slices obtained from a CT (Computed Tomography) scan are gray scale representations of the absorption map in a defined plane. In this respect, the different gray-scale levels identify the variation of the absorption capability from the materials in the bulk. In the reference tomography used in this paper, the pixel values span from the dark color of the air medium (baseline for minimal-absorption) to the light-gray color of the phase-stabilized ammonium nitrate. Brighter spots could be observed in presence of metal (most opaque material), as seen in Fig. 1.

### 6.2 Unsharpness issue

The contact between two materials featured by different X-ray opacity is identified by the shift of the gray scale value across two interfacing voxels. The variation should be point-wise in the case of ideal behavior whereas a real tomography is characterized by smooth transition. A 2D reconstruction of the issue is reported in Fig. 4. The lack of localized gray-scale change makes the border reconstruction unsharp, causing an initial uncertainty on the particle surface position. Main sources contributing to the generation of unsharpness phenomenon consist of scanning geometry, system limits, and movement imperfections. In the first case, the effect is caused by the interaction between non-infinitesimal size of the X-ray source and magnification factor, which in turn depends on the reciprocal position of source, sample, and X-ray detector. The second case is a direct consequence of the pixel resolution of the X-ray detector. The third case is generated by issues of the sample fixing and accuracy of the moving mechanism.

Literature papers identify four primitives for edge representation in tomographic reconstructions They are reported in Fig. 5. In an ideal case, a step-kind signal would identify the border as two materials featuring different X-ray absorption properties are in direct contact. In Fig. 6, a particle was targeted (id. case number 001). A probing line was randomly chosen and the grey-scale values were captured. Uncertainty identification of the edge is clear on the sides of the particle as the gray-scale value does not pass through a sharp border but smooth transition between air and particle bulk is observed making it similar to a ramp. The transition is quite smooth and takes more than 50 μm long on both sides of a particle having a diameter of about 400 μm. The analysis was extended to other particles in the bulk with a stochastic approach. The global unsharpness estimation was identified monitoring the convergence of mean and standard deviations which both converged after 180 measurements to respectively 54.0(56) μm and 3.0(034) μm. The value of the unsharpness is connected to the capacity of correct edge identification and proper estimation of particle

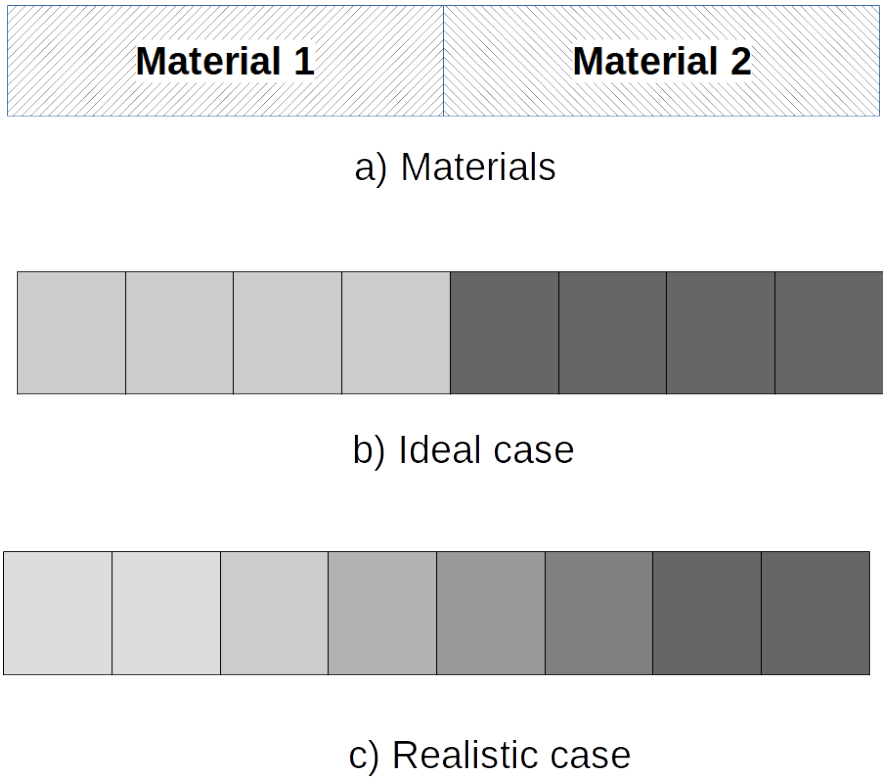


Figure 4: Tomographic interface representation

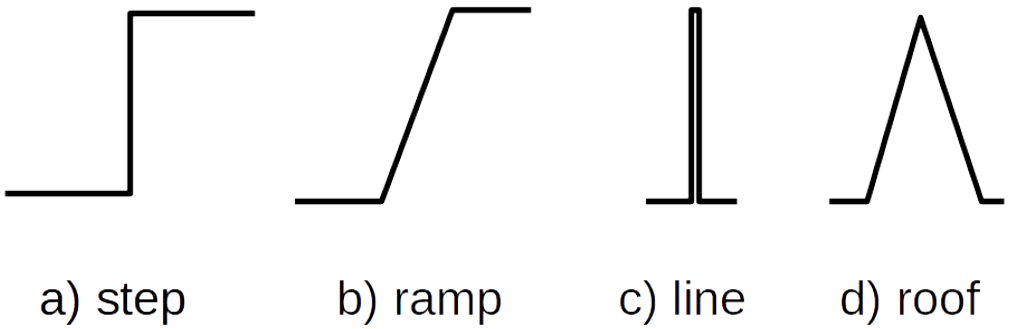


Figure 5: Types of edges in image analysis[23]

volume. The value of the standard deviation is quite limited and shows that the property is quite uniform across the reconstructed volume.

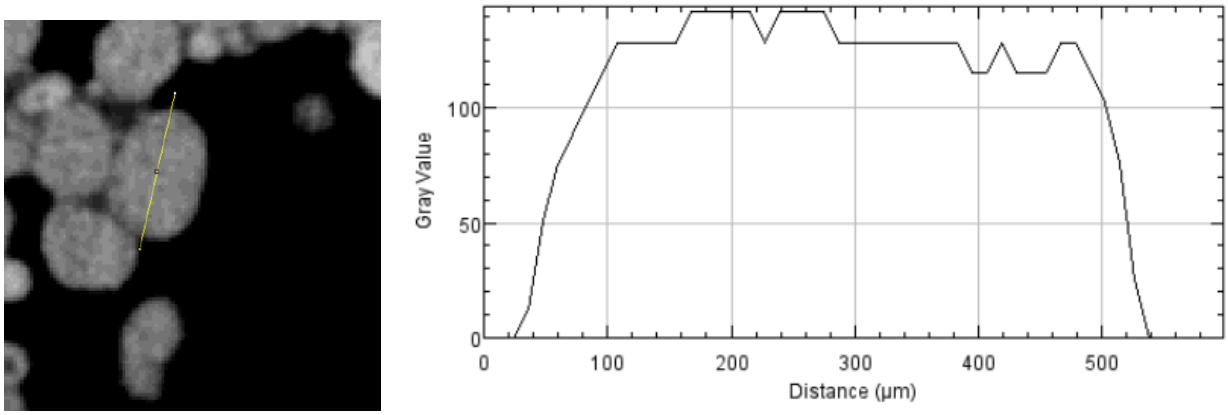


(a) Probing segment in a propellant tomography

(b) Gray scale profile along the probing segment

Figure 6: Example of edge unsharpness (Case 001).

### 6.3 Noise and sharpness

The bulk of uniform materials should feature constant gray scale level. For example, the beam hardening creates a shift of the absorption map and virtually uniform material appear with a gradual variation of the gray-scale when moving towards from the center towards the external surface. This artifact is characterized by smooth alteration of the image, can be easily treated through corrections, and does not interfere too much with the identification of the single particles. The noise introduced by the sensor-source interaction is a short-range disturbance. It is characterized by a variation at pixel level. Within the particle bulk it is represented by a high-frequency spatial noise, overlapped to the general gray-scale value. Int he next images, said interval is referred to as "oscillation region". The plot for the Case-001 particle shows a very modest fluctuation of the bulk value within the borders of the particle. A quantitative analysis of the plot is reported in 7. The unsharpness is different at the two edges but the bulk properties are quite uniform, despite some minor modification.

From the same tomography, a different probing line is plot over two contacting particles (id. Case-025). The tomography magnification and the gray-scale plot are reported in Fig. 8. From the 2D slice, it appears that a small gap filled with binder is present in between and the line is traced on purpose across that interface. On the other side, the particle faces a void. As expected, in the gray-scale plot the two particles are separated by a minimum of the absorption map but the value is higher than the one associated to vacuoles. The reason is twofold. On the one side, the binder is not completely transparent to X-rays. On the other side, the contact involves a limited number of voxels, causing possible noise and resolution effects.

Denoising and sharpness are very often treated together because methods to highlight borders generally can also amplify the image noise. The issue is here studied by convolving the region of interest with a combination of Gaussian blur and unsharp mask 3D kernels. One lateral particle of the reference tomography is targeted (particle id. "Case-059"). For simplicity, the probing line is considering only a single item and does not intersect other borders. Figure 9 is showing the application of the filters to the slice having the largest particle section area on it. The plot-over-line probing is reported in Fig. 10. Main observations can be conducted in the central oscillation region and on the two particle borders.

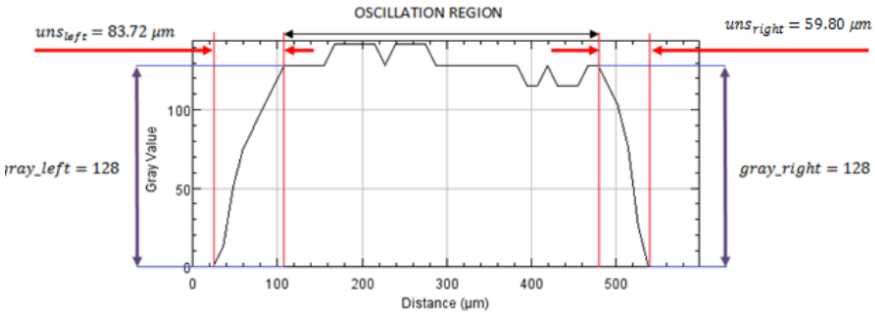


Figure 7: Interpretation of Case-001 particle gray-scale profile

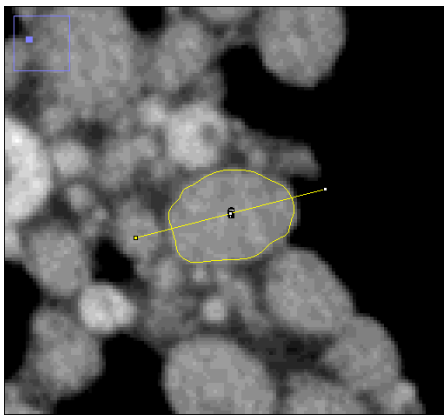

(a) Probing line

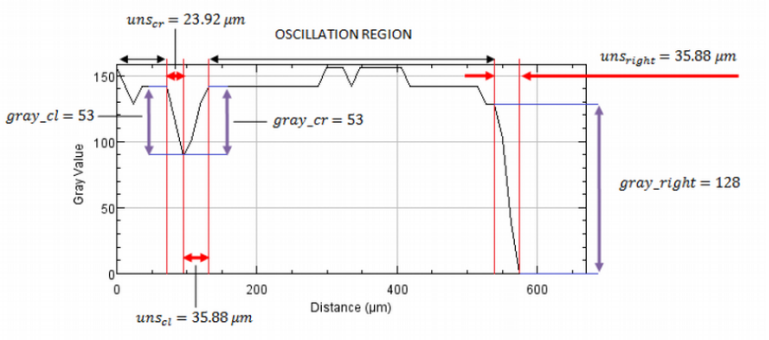


(b) Gray-scale value

Figure 8: Image of particle "Case-025" with yellow probing line

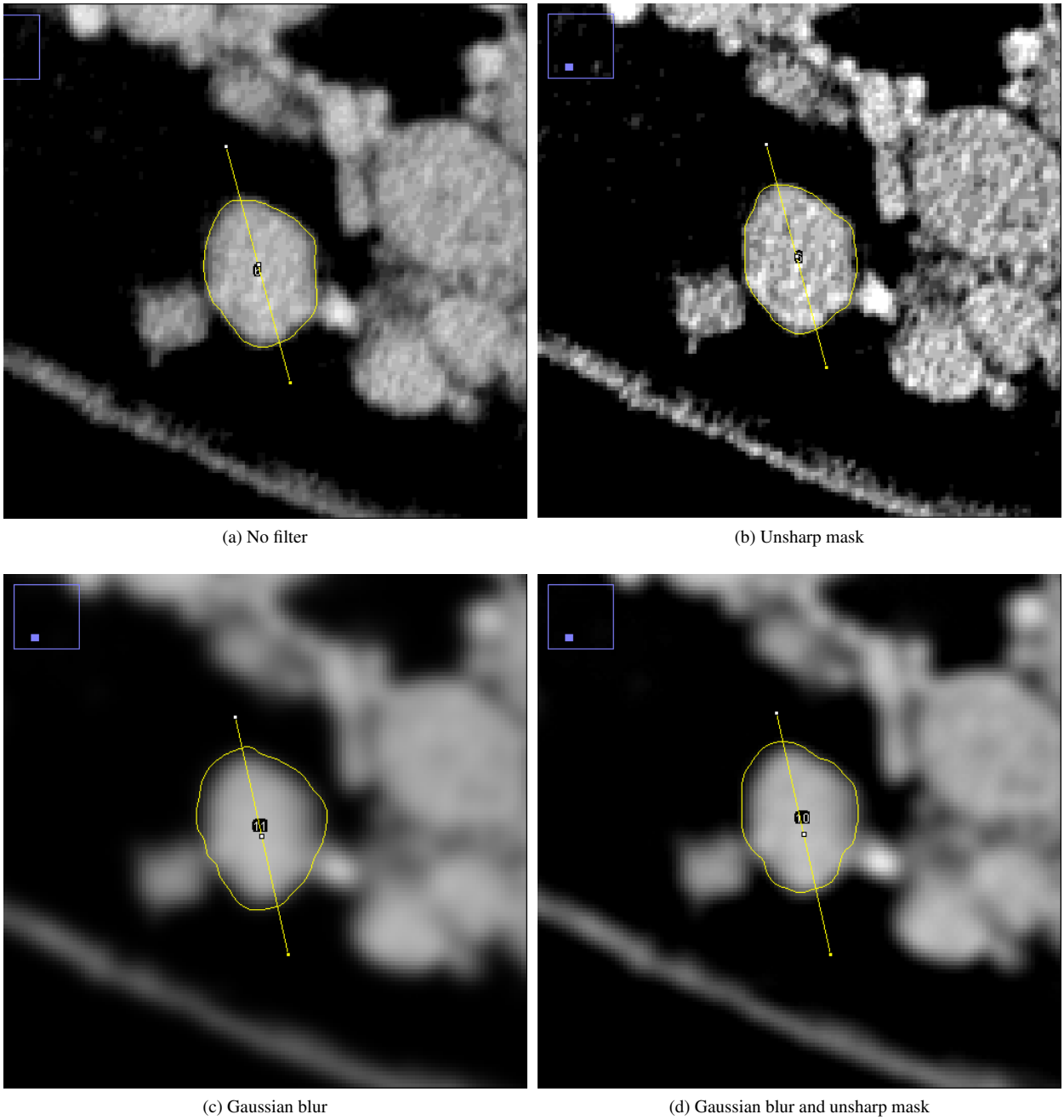

(a) No filter

(b) Unsharp mask

(c) Gaussian blur

(d) Gaussian blur and unsharp mask

Figure 9: Image of particle "Case-059" after image processing

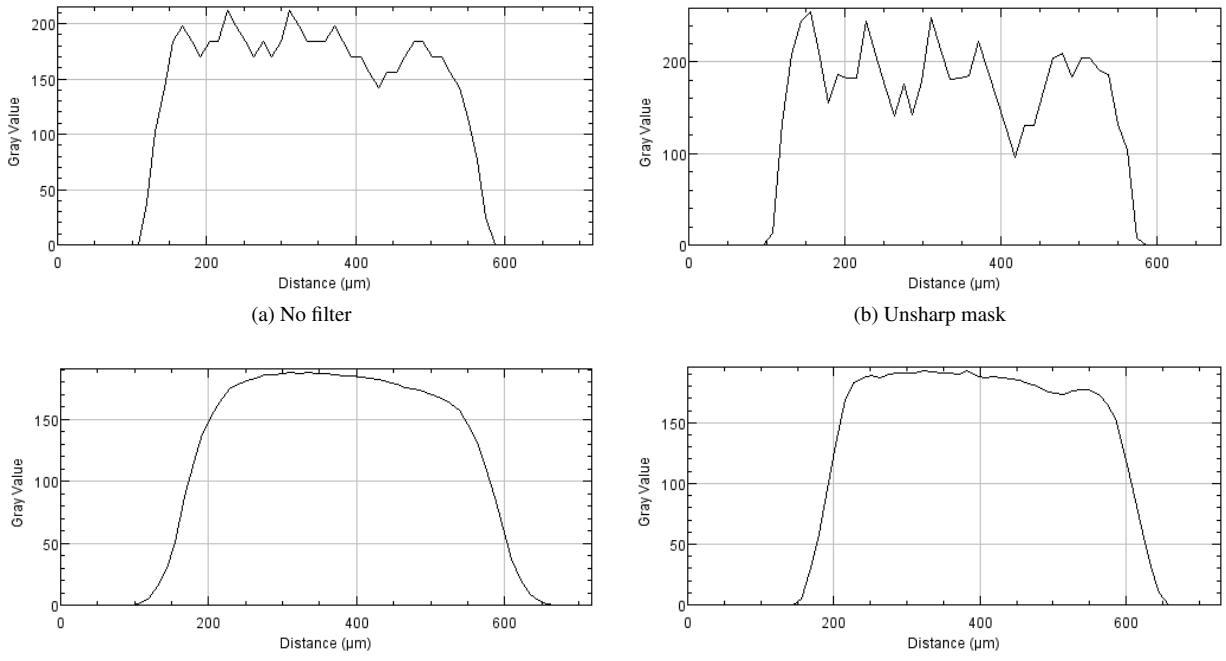


(a) No filter

(b) Unsharp mask

(c) Gaussian blur

(d) Gaussian blur and unsharp mask

Figure 10: Gray-scale values on probing line of particle "Case-059" after image processing

The unsharp mask filtering (case b, radius = 2 pixels) makes the border more defined. Qualitative observation of the image shows more contrast with respect to the initial picture. From a quantitative viewpoint, the gray-scale probing plot features sharper side values and more noise. For example, the left edge reduces the rising interval from about 75 μm to about 50 μm. The measure was picked up from the zero level to the first maximum. In the oscillation region data fluctuation grows from a maximum of 60 max-min difference of gray-scale units to about 160. The reader should notice that the highest value of the curve is actually higher than $2^8$ (the number of gray levels for the original tomography) because it results from the unbounded application of a mathematical formula. The minimum located about the coordinate 400 μm is pronounced and may be considered an edge by eventual automated identification procedure.

The Gaussian filter (case c, $\sigma = 2$ pixels) produces a blurred image. The contours become confused and the contrast decreases. The bulk of particles becomes more uniform. As a result in the gray-scale signal the edge of the particle covers a larger range, quantified in about 125 pixels from zero level to the end of the rise identified by the double-tangent method. On the other hand, the oscillation region disappears completely.

The sequential combination of Gaussian blur and unsharp mask (case d) is a method that acts as compromise between denoising and feature highlighting. Apparently the image is similar to the one produced by the Gaussian blur. Particle bulk appears uniform and edges seem to be blurry. The difference is clear only after the analysis of the gray-scale plot-over-line data. The left-side border of the particle is identified by a rise of about 75 units of the gray-scale value, similar to the origial image. Strong difference is observed in the particle bulk where almost uniform profile is obtained and the max-min shift is about 20 units. In this specific case, this image allows better identification than the original one because maintains similar border unsharpness and removes the variations in the oscillation region, which may be interpreted as borders of touching particles.

## 7. Final remarks

An example of microstructure analysis has been shown in this paper. Whereas qualitative interpretation is easy and straightforward, difficulties arise when the analysis intends to extract quantitative information from the scanned. The proper identification of the particles becomes the first and most important step, obtaining reliable information on surface and volume. In this respect this paper has addressed only one aspect relevant to data quality and improvement methods of the data set.

The current algorithms developed at the Space Propulsion Laboratory (SPLab-POLIMI) are still experimental and in most of the cases are manual. The heterogeneous nature of these materials require statistical approaches for proper characterization, requiring high number of samples. In this respect both the processing effort and the introduction of the human factor are limitations that should be targeted by future improvements of the technique.

## Acknowledgments

This work is a joint research effort between the Space Propulsion Laboratory (SPLab-POLIMI) and the Advanced Manufacturing Laboratory (AMALA), both part of Politecnico di Milano.

## References

[1] N. S. Cohen. A pocket model for aluminum agglomeration in composite propellants. *AIAA Journal*, 21(5):720–725, 1983.

[2] F. Maggi, L. T. DeLuca, and A. Bandera. Pocket model for aluminum agglomeration based on propellant microstructure. *AIAA Journal*, 53(11):3395–3403, 2015.

[3] R. K. McGeary. Mechanical packing of spherical particles. *Journal of the American Ceramic Society*, 44(10):513–522, 1961.

[4] F. Maggi, S. Stafford, and T. L. Jackson. Nature of packs used in propellant modeling. *Physical Review E*, 77(046107):1–17, 2008.

[5] P. Le Breton and D. Ribéreau. Casting process impact on small-scale solid rocket motor ballistic performance. *Journal of Propulsion and Power*, 18(6):1211–1217, 2002.

[6] F. Maggi, L. T. De Luca, A. Bandera, V. S. Subith, and A. Annovazzi. Burn-rate measurement on small-scale rocket motors. *Defence Science Journal*, 56(3):353–367, July 2006. DESIDOC 4100 5223 PUB.

[7] X. Wang, J. Buckmaster, and T. L. Jackson. Burning of ammonium perchlorate ellipses and spheroids in fuel binder. *Journal of Propulsion and Power*, 22(4):764–768, 2006.

[8] S. R. Stock. X-ray computed tomography. In E. N. Kaufmann, editor, *Characterization of Materials*, pages 1624–1641. John Wiley & Sons, 2012.

[9] S. Gallier. Microstructure of composite propellants using simulated packings and x-ray tomography. *Journal of Propulsion and Power*, 24(1):154–157, 2008.

[10] B. Collins, F. Maggi, K. Matous, T. L. Jackson, and J. Buckmaster. Using tomography to characterize heterogeneous propellants. *AIAA paper*, 2008-941, 2008.

[11] F. Maggi and P. Garg. Fragmentation of ammonium nitrate particles under thermal cycling. *Propellants, Explosives, Pyrotechnics*, 43:315–319, 2018.

[12] L. W. Goldman. Principles of CT: Radiation dose and image quality. *Journal of Nuclear Medicine Technology*, 35(4):213–225, dec 2007.

[13] S. Schlüter, A. Sheppard, K. Brown, and D. Wildenschild. Image processing of multiphase images obtained via X-ray microtomography: a review. *Water Resources Research*, 50(4):3615–3639, 2014.

[14] Ning R., X. Tang, and D. Conover. X-ray scatter correction algorithm for cone beam CT imaging. *Medical Physics*, 31(5):1195–1202, apr 2004.

[15] R.S. Maia, C. Jacob, A.K. Hara, A.C. Silva, W. Pavlicek, and M.J. Ross. An algorithm for noise correction of dual-energy computed tomography material density images. *International Journal of Computer Assisted Radiology and Surgery*, 10(1):87–100, may 2014.

[16] M. Al-Frejat and M. HjoujBtoush. A new approach for enhancing the quality of medical computerized tomography images. *International Journal of Advanced Computer Science and Applications*, 7(5), 2016.

[17] Bu¨lent Sankur. Survey over image thresholding techniques and quantitative performance evaluation. *Journal of Electronic Imaging*, 13(1):146, jan 2004.

[18] T. R. Latharani, M. Z. Kurian, and M. V. Chidananda Murthy. Various object recognition techniques for computer vision. *Journal of Analysis and Computation*, 7(1):39–47, 2011.

[19] P. J. Barrett. The shape of rock particles, a critical review. *Sedimentology*, 27(3):291–303, 1980.

[20] M. Bartscher, U. Neuschaefer-Rube, J. Illemann, F. Borges de Oliveira, A. Stolfi, and S. Carmignato. Qualification and testing of CT systems. In S. Carmignato, W. Dewulf, and R. Leach, editors, *Industrial X-Ray Computed Tomography*, chapter 6, pages 185–228. Springer International Publishing, 2018.

[21] G. Moroni and S. Petrò. A discussion on performance verification of 3D X-ray computed tomography systems. *Procedia CIRP*, 75:125–130, 2018.

[22] C. Martinez-Ortiz. *2D and 3D Shape Descriptors*. PhD thesis, University of Exeter, 2010.

[23] R. Jain, R. Kasturi, and B. G. Schnuck. *Machine Vision*. McGraw-Hill, 1995.